

Determination of the activity of hydrogen peroxide scavenging by using blue-emitting glucose oxidase–stabilized gold nanoclusters as fluorescent nanoprobe and a Fenton reaction that induces fluorescence quenching

Wanwan Cui¹ · Haiyan Qin¹ · Yang Zhou¹ · Jianxiu Du¹

Received: 26 August 2016 / Accepted: 27 January 2017 / Published online: 6 February 2017
© Springer-Verlag Wien 2017

Abstract The authors describe a rapid and sensitive method for the determination of the activity of scavenging hydrogen peroxide in which glucose oxidase–stabilized gold nanoclusters (AuNCs) were employed as a fluorescent nanoprobe. The AuNCs are synthesized by a biomineralization process and display an intense blue fluorescence peaking at 450 nm and a quantum yield of 1.1% under 360–nm excitation. The Fenton reaction induces quenching of fluorescence, and this effect can be used to determine H₂O₂ in the 0.5 to 10 μmol·L⁻¹ concentration range. The substances displaying H₂O₂ scavenging activity prevent quenching and thus restore fluorescence. The intensity of restored fluorescence is directly related to the H₂O₂ scavenging activity of the antioxidant. The method was applied to the determination of the H₂O₂ scavenging activity of the model antioxidants ascorbic acid and tartaric acid which gave IC₅₀ values of 7.4 and 19.1 μmol·L⁻¹, respectively.

Keywords Hydrogen peroxide · Scavenging activity · Gold nanoclusters · Glucose oxidase · Biomineralization · Fluorescent nanoprobe · Fenton reaction

Electronic supplementary material The online version of this article (doi:10.1007/s00604-017-2110-x) contains supplementary material, which is available to authorized users.

✉ Jianxiu Du
jxdu@snnu.edu.cn

¹ Key Laboratory of Analytical Chemistry for Life Science of Shaanxi Province, School of Chemistry and Chemical Engineering, Shaanxi Normal University, Xi'an 710062, China

Introduction

Reactive oxygen species (ROS) such as hydrogen peroxide (H₂O₂), superoxide anion (O₂^{•-}), and hydroxyl radical (•OH) play important roles as the mediators involved in signaling pathways to maintain cellular homeostasis [1–3]. On the contrary, these ROS may induce severe oxidative injury, resulting in a variety of damages [4–6]. Among biologically relevant ROS, H₂O₂ is a non-radical oxidizing species. It can be generated in vivo under physiological condition by peroxisome, oxidative enzyme, or the dismutation of superoxide radical catalyzed by superoxide dismutase [7]. H₂O₂ has been confirmed as a major messenger molecule in various redox-dependent cellular signaling transductions with low reactivity and high intracellular concentration [8, 9]. If present in excess under stress conditions, H₂O₂ can induce oxidative damage of many cellular components. H₂O₂ can be converted into other ROS, such as •OH, the most potent and reactive ROS species, which causes the oxidative degradation of biological macromolecules such as lipid, protein, carbohydrate and nucleic acid [10, 11]. Therefore, the determination of H₂O₂ scavenging activity has become important for evaluation of reactive oxygen scavenging activity.

H₂O₂ scavenging activity is usually determined by direct monitoring the intrinsic absorption of H₂O₂ at 230 nm in the UV region. Nevertheless, in most case, the sample may also absorb at this wavelength that influences the precision and accuracy [12]. An alternative assay was HRP-based detection system, in which HRP catalyzed the oxidation of colorimetric [13] or fluorogenic [14] substrates. Unfortunately, peroxidase can also react with certain substrate in the absence of H₂O₂ [15]. Another detection method was relied on peroxyoxalate chemiluminescence reaction [16, 17]. This system can only be used to evaluate lipophilic antioxidants because of the non-

polar environment employed. Recently, Qian group developed a nanoparticle-based approach for estimating H_2O_2 scavenging activity based upon H_2O_2 inducing the formation of gold nanoshells on SiO_2 cores that altered the corresponding plasmon absorption band [18] or surface-enhanced Raman scattering [19].

Fluorescent gold nanoclusters (AuNCs) are a fascinating class of nanomaterials that are composed of several to tens of atoms. They exhibit molecule-like property and produce size-dependent fluorescence. The fluorescent AuNCs have been extensively applied in biosensing, bioimaging, enzyme activity assay, and protein discrimination [20]. Among the various synthetic approaches, proteins-directed synthesis of fluorescent AuNCs under mild and green condition is of very attractive [21]. Different proteins-directed, e.g. bovine serum albumin (BSA) [22], insulin [23], pepsin [24], and horseradish peroxidase (HRP) [25], L-amino acid oxidase [26], fluorescent AuNCs have been successfully prepared. Glucose oxidase (GOx) is a dimeric glycoprotein consisting of two identical subunits with flavin adenine dinucleotide as moiety. The molecular weight of GOx ranges from approximately 130 to 175 kDa [27]. The presence of cysteine residues in molecule structure makes GOx become the potential template to direct synthesis of fluorescent AuNCs. Xia et al. reported a red fluorescent AuNCs by using tetrakis (hydroxymethyl) phosphonium-capped gold nanoparticle as the precursor and thioctic acid-functionalized GOx as the etchant, respectively [28]. The procedure for the preparation of AuNCs was slightly complex.

In this work, a blue-emitting fluorescent AuNCs stabilized by GOx was prepared via a one-pot biomineralization process under wide pH ranges (pH 5–12). Although protein-directed fluorescent AuNCs with red emission were frequently reported, the synthesis of other color fluorescent AuNCs with proteins-directed approach was very rare [24, 29]. We observed that Fenton reaction can induce a significant fluorescence quenching of the prepared AuNCs. This system was further explored to estimate the scavenging activity of H_2O_2 .

Experimental

Chemicals

All chemicals were of analytical grade and used without further purification. Ultrapure water was produced from Molegene 1810b ultrapure water system (<http://www.molwater.com>, Chongqing Mole, China). Glucose oxidase (GOx, 128,200 units·g⁻¹) from *Aspergillus niger* was purchased from Sigma-Aldrich Co. LLC. (<http://www.sigmaaldrich.com>, United Kingdom). Hydrogen tetrachloroaurate tetrahydrate ($\text{HAuCl}_4 \cdot 4\text{H}_2\text{O}$) was obtained from Shanghai Chemical Reagent Co., Ltd. (<http://www.shiyicr.com.cn>, Shanghai, China). Hydrogen peroxide

(H_2O_2 , 30%) was purchased from Xilong Chemical Co., Ltd. (<http://xlhg.company.lookchem.cn>, Sichuan, China). Ammonium iron (II) sulfate[(NH_4)₂Fe(SO₄)₂·6H₂O] and ascorbic acid were purchased from Xi'an Chemical Reagent Factory (<http://www.crc-xa.com>, Xi'an, China). Tartaric acid was purchased from Beijing Chemical Reagent Company (<http://www.crc-bj.com>, Beijing, China).

Apparatus

Fluorescence spectra were recorded on an F-2700 fluorescence spectrophotometer (<http://www.hitachi-hightech.com>, Hitachi, Japan) by using a 200- μL cuvette. Both the slit widths for excitation and emission were set at 10 nm and the high voltage of the photomultiplier tube was biased at 700 V. Ultraviolet-visible (UV-vis) absorption spectra were recorded on a TU-1901 double-beam UV-vis spectrophotometer (<http://www.pgeneral.com>, Beijing Purkinje General Instrument Co Ltd., China) with a 10 mm cuvette. X-ray photoelectron spectroscopy (XPS) spectra of the AuNCs were measured with an Axis Ultra-Imaging Photoelectron Spectrometer (<http://www.kratos.com>, Kratos Analytical Ltd., England). Infrared spectra of GOx and the AuNCs with KBr pellets were collected by using a Tensor 27 spectrophotometer (<https://www.bruker.com>, Bruker, Germany). The circular dichroism (CD) spectra of GOx and the AuNCs were obtained on Chirascan-circular dichroism spectrometer (www.photophysics.com/cn, Applied Photophysics Limited Company, United Kingdom). Transmission electron microscopy (TEM) images of the AuNCs were measured by using a JEM-2100 transmission electron microscope (<http://www.jeol.co.jp/cn>, JEOL Ltd., Japan) with an accelerating voltage of 200 kV.

Synthesis of the AuNCs

All glassware were soaked in aqua regia (HNO_3/HCl , 1:3) for 24 h, rinsed thoroughly with water, and then dried for use. The procedure for the preparation of the AuNCs was similar to the protocol of Xie's [22] with some modification. Briefly, aqueous HAuCl_4 solution (12 mmol·L⁻¹, 2.5 mL, 37 °C) was added into GOx solution (60 mg·mL⁻¹, 2.5 mL, 37 °C) under vigorously stirring. After adjusting the pH to ~5, the solution was allowed to react at 37 °C for 15 h. The resultant solution was dialyzed for 24 h in membrane tubing with a molecular weight cutoff of 3000 Da to remove any impurities. The prepared AuNCs was stored at 4 °C in a refrigerator when not used.

Procedure for H_2O_2 detection

For the detection of H_2O_2 , 70 μL of H_2O_2 solution and 30 μL of Fe^{2+} solution (2.0 mmol·L⁻¹) were added into 500 μL of 1:25 dilution the AuNCs solution (prepared in 12 mmol·L⁻¹ HAC-NaAc buffer, pH 4.50). After incubating at ambient

temperature for 5 min, the fluorescence spectrum of the resultant solution was measured upon excitation at 360 nm.

Procedure for H₂O₂ scavenging activity assay

For the assay of H₂O₂ scavenging activity, 40 μL of antioxidant solution, 30 μL of H₂O₂ solution (0.2 $\text{mmol}\cdot\text{L}^{-1}$) and 30 μL Fe²⁺ solution (2.0 $\text{mmol}\cdot\text{L}^{-1}$) were successively added into 500 μL of 1:25 dilution the AuNCs solution (prepared in 12 $\text{mmol}\cdot\text{L}^{-1}$ HAc–NaAc buffer, pH 4.50). The mixed solution was incubated at ambient temperature for 5 min and then scanned the fluorescence spectrum with fixing excitation wavelength at 360 nm.

Results and discussion

Preparation and characterization of the AuNCs

The AuNCs was prepared via a “one-pot” biomineralization approach. HAuCl₄ solution and GOx solution were mixed and reacted at 37 °C at pH 5 for 15 h. During the reaction, the color of the solution changed from light yellow to dark yellow. As shown in Fig. S1, curve c, the absorbance of the AuNCs at 272 nm decreased from 1.126 to 0.738; while at 382 nm had a slight increase (from 0.054 to 0.085) after the reaction. These results indicated that the structure of the polypeptide chains and FAD moiety in GOx molecule changed during the reaction. No surface plasma resonance peak at 520 nm emerged on the absorption spectrum of the reaction mixture, suggesting that the size of the Au nanoparticles was less than 2 nm [30].

GOx solution featured a fluorescence peak at about 530 nm with excitation at 360 nm (Fig. 1a, curve a, a'), owing to FAD intrinsic fluorescence [31]. After the reaction, the fluorescence band of FAD slightly blue-shifted from 530 nm to 517 nm and a new fluorescence peak appeared at about 450 nm under the excitation at 360 nm (Fig. 1a, curve b, b'), the characteristic of AuNCs. The fluorescence quantum yield (QY) of the AuNCs was about 1.1% by using quinine sulfate as a reference (QY 0.55).

TEM image was conducted in order to obtain the information on the size and surface morphology of the AuNCs. Unfortunately, no TEM image was obtained probably because the size of the AuNCs was too small to fell out of the capability of TEM. It was reported that the emission wavelength of fluorescent AuNCs was strongly dependent on the size of the AuNCs cores [24, 32]. The smaller sizes of the AuNCs have; the shorter wavelengths of the fluorescence emit. The fluorescence peak of the AuNCs was very close to that of Au₈NCs [24, 30]. Thus, it was deduced that the AuNCs might consist of about eight gold atoms with an average size of less than 1 nm.

X-ray photoelectron spectroscopy (XPS) was carried out to explore the valence and composition of the AuNCs. As

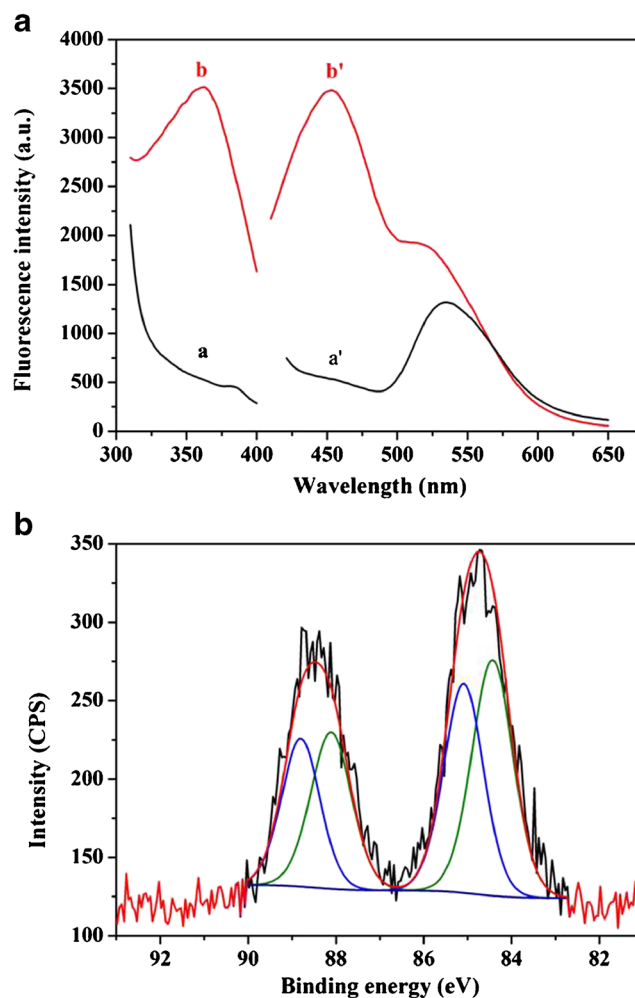


Fig. 1 **a** The fluorescence excitation and emission spectra of (a, a') pure GOx and (b, b') the AuNCs and **b** XPS spectra of the AuNCs. The original spectrum is in black, the Au(I) 4f spectrum after analysis is in red, the Au(I) 4f spectrum after analysis is in blue, and the Au(0) 4f spectrum after analysis is in green

shown in Fig. 1b, the XPS spectrum showed Au 4f band of binding energy at 88.48 and 84.73 eV, assigned to Au 4f_{5/2} and Au 4f_{7/2} peaks, respectively. They were further deconvoluted into two distinct components: 84.44 eV (Au 4f_{7/2}) and 88.11 eV (Au 4f_{5/2}), typical of Au(0), and 85.09 eV (Au 4f_{7/2}) and 88.80 eV (Au 4f_{5/2}), characteristic for Au(I) [33], respectively. The best fit of the data indicated that the AuNCs consists of approximately 53.5% of Au(0) in the core and 46.5% of Au(I) at the core surface, which might stabilize the AuNCs.

Figure S2 shows the infrared spectra of pure GOx and the AuNCs. The same peak bands appeared on the infrared spectra of pure GOx and the AuNCs, indicating that GOx was successfully capped on the surface of the AuNCs.

Figure S3 shows the circular dichroism (CD) spectra of GOx before and after the reaction. The results indicated that the secondary structure of GOx changed from α -helix to β -sheet structure after the reaction.

The pH of the reaction influences the formation and the size of AuNCs [22, 24]. We attempted to prepare the AuNCs under weak acidic (pH 5), neutral (pH 7), and strong basic (pH 12). The AuNCs can be prepared under the examined pH conditions (pH 5–12). The maximum emission wavelengths are the same and independent on the pH of the reaction employed (Fig. S4), indicating that they had the same size. This was different with that of the pepsin-mediated the preparation of AuNCs, in which the maximum emission wavelength and size of AuNCs were strongly dependent on the pH of the reaction employed [26]. Finally, the AuNCs was prepared at pH 5 since it had the highest emission intensity.

The fluorescence intensity of the AuNCs was also dependent on the reaction time. Fig. S5 shows the fluorescence intensity reached a plateau when the reaction time was longer than 15 h. Therefore, 15 h was employed for the preparation of the AuNCs.

Fenton reaction-mediated fluorescence quenching of the AuNCs

Not like other AuNCs, such as BSA-stabilized AuNCs [34] and HRP-stabilized AuNCs [25], H_2O_2 alone cannot cause an observable fluorescence quenching on the AuNCs (Fig. 2, curve b). Bearing in mind that $\cdot\text{OH}$ is more oxidative and can be formed by the reaction of H_2O_2 with Fe^{2+} as a catalyst (Fenton reaction). As expected, the fluorescence of the AuNCs was dramatically quenched when introducing $100 \mu\text{mol}\cdot\text{L}^{-1}$ Fe^{2+} into the reaction system (Fig. 2, curve d). As the control, the influence of the same amount of Fe^{2+} was also examined. As shown in Fig. 2, curve c, the fluorescence of the AuNCs showed no significant change in the presence of Fe^{2+} alone, ruling out the quenching effect from Fe^{2+} itself.

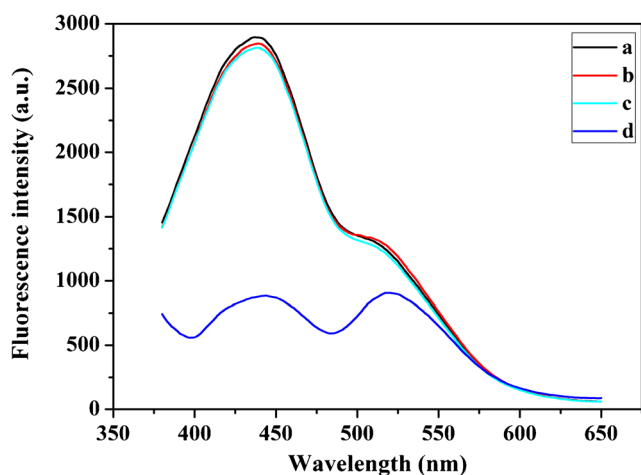


Fig. 2 Fluorescence emission spectra of (a) 1:30 dilution Au NCs in the presence of (b) $50.0 \mu\text{mol}\cdot\text{L}^{-1}$ H_2O_2 , (c) $100 \mu\text{mol}\cdot\text{L}^{-1}$ Fe^{2+} , and (d) $50.0 \mu\text{mol}\cdot\text{L}^{-1}$ H_2O_2 and $100 \mu\text{mol}\cdot\text{L}^{-1}$ Fe^{2+} in $10 \text{mmol}\cdot\text{L}^{-1}$ HAC–NaAc buffer (pH 5.0)

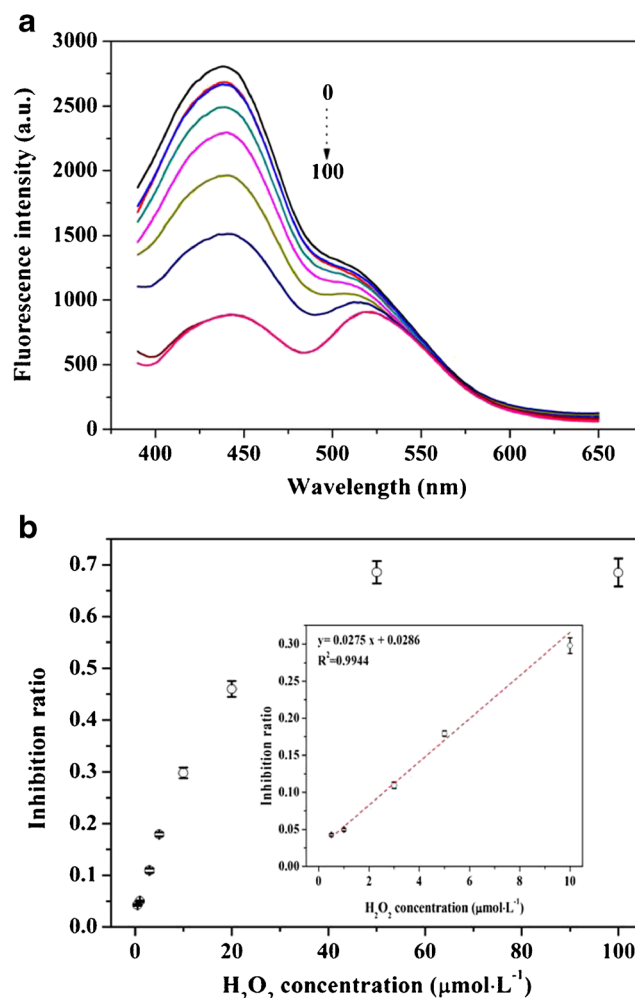


Fig. 3 a Fluorescence emission spectra of the AuNCs in the presence of different concentrations of H_2O_2 ($\mu\text{mol}\cdot\text{L}^{-1}$) and b calibration plot of inhibition ratio to H_2O_2 concentration. 1:30 dilution AuNCs, $100 \mu\text{mol}\cdot\text{L}^{-1}$ Fe^{2+} , $10 \text{mmol}\cdot\text{L}^{-1}$ HAC–NaAc buffer (pH 4.5)

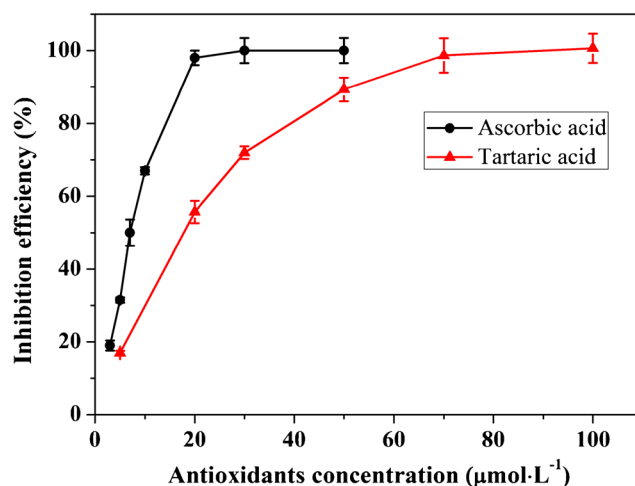


Fig. 4 The inhibitory efficiency as a function of antioxidant concentrations added. 1:30 dilution AuNCs, $10.0 \mu\text{mol}\cdot\text{L}^{-1}$ H_2O_2 , $100 \mu\text{mol}\cdot\text{L}^{-1}$ Fe^{2+} , $10 \text{mmol}\cdot\text{L}^{-1}$ HAC–NaAc buffer (pH 4.5)

Table 1 Hydrogen peroxide scavenging activity (SA_{HP}) of the antioxidants tested

Antioxidant	IC_{50} ($\mu\text{mol}\cdot\text{L}^{-1}$)	SA_{HP}
Ascorbic acid	7.41 ± 0.54	0.13 ± 0.01
Tartaric acid	19.13 ± 1.07	0.052 ± 0.003

Results are mean of triplicate determination \pm S.D.

SA_{HP} is expressed as $(\mu\text{mol}\cdot\text{L}^{-1})^{-1}$ ($1/IC_{50}$)

This system was expected to explore as a fluorescent nanoprobe for H_2O_2 . To achieve the maximum sensitivity, the following parameters were optimized: the dilution ratio of the AuNCs, the Fe^{2+} concentration, the kind and pH of the buffer, and the reaction time. Inhibition ratio, calculated as $(F_b - F)/F_b$, was employed for the optimization, where F_b and F were the fluorescence intensity at 450 nm in the absence and the presence of H_2O_2 upon excitation at 360 nm. Respective data and Figures are given in the Electronic Supporting Material (Fig. S6–S10). The following experimental conditions were found to give best results: 1:30 dilution ratio AuNCs, $100 \mu\text{mol}\cdot\text{L}^{-1}$ Fe^{2+} , $10 \text{ mmol}\cdot\text{L}^{-1}$ HAC–NaAc buffer (pH 4.5), and 5 min of reaction time.

Under the selected experimental conditions, the response of the system to different concentrations of H_2O_2 was investigated. As shown in Fig. 3a, the fluorescence intensity at 450 nm gradually decreased with increasing the concentration of H_2O_2 . A linear relationship between the inhibition ratio and the concentration of H_2O_2 was observed in the range of 0.5 – $10.0 \mu\text{mol}\cdot\text{L}^{-1}$ (inset of Fig. 3b). The linear regression equation can be expressed as $(F_b - F)/F_b = 0.0275 c (\mu\text{mol}\cdot\text{L}^{-1}) + 0.0286$ with a coefficient of regression (r^2) of 0.9944. The detection limit was determined to be $0.23 \mu\text{mol}\cdot\text{L}^{-1}$ H_2O_2 . The relative standard deviation was 1.1% for eleven replicate measurements of $1.0 \mu\text{mol}\cdot\text{L}^{-1}$ H_2O_2 solution, indicating better precision of the system for the detection of H_2O_2 .

Evaluation of H_2O_2 scavenging activity

This system was further applied for evaluating H_2O_2 scavenging activity (SA_{HP}). The SA_{HP} of two common antioxidants,

ascorbic acid and tartaric acid, were investigated. With the presence of antioxidant, H_2O_2 with $10.0 \mu\text{mol}\cdot\text{L}^{-1}$ original concentration would be partly scavenged and the fluorescence quenching of the AuNCs would be prohibited, resulting in a restore in fluorescence intensity. The scavenging efficiency was calculated as $(F_b - F_i)/(F_b - F)$, where F_b was the fluorescence intensity of the AuNCs in the absence of H_2O_2 , and F and F_i were fluorescence intensity of the AuNCs in the presence of $10.0 \mu\text{mol}\cdot\text{L}^{-1}$ H_2O_2 without and with adding the antioxidants. Fig. 4 showed the scavenging efficiency plotting against the concentration of antioxidants added. The amount of each antioxidant to provoke 50% scavenging efficiency was taken as IC_{50} . The SA_{HP} was obtained as $1/IC_{50}$ and expressed as $(\mu\text{mol}\cdot\text{L}^{-1})^{-1}$. Table 1 summarized the IC_{50} value and SA_{HP} for ascorbic acid and tartaric acid, respectively. Ascorbic acid had higher H_2O_2 scavenging activity than that of tartaric acid. This result was consistent with the previous publication, indicating the method can be used to evaluate H_2O_2 scavenging activity. Table 2 overviews the recently reported methods for H_2O_2 scavenging activity assays. As can be seen, the sensitivity of our method was higher than that of most reported methods [12–14] and comparable to that of the chemiluminescence method [16] and SERS [19].

Conclusions

In summary, a blue-emitting AuNCs was successfully prepared by using GOx as both the reducing and stabilizing agents through a biomineralization process. The fluorescence of the AuNCs was significantly quenched by H_2O_2 in the presence of Fe^{2+} as the catalyst. The procedure allowed to the measurement of H_2O_2 in the concentration range of 0.5 – $10 \mu\text{mol}\cdot\text{L}^{-1}$. The method was further used for evaluating H_2O_2 scavenging activity of antioxidants due to their restoring the fluorescence. The restored fluorescence intensity was closely related to the H_2O_2 scavenging activity of the antioxidants. The application of the method was evaluated by employing ascorbic acid and tartaric acid as the model antioxidants. Our method is simple, sensitivity, will open a new way for evaluating other antioxidants.

Table 2 Comparison of recently reported methods for H_2O_2 scavenging activity assays

Methods	Chemical used	Figures of merit	Ref.
Spectrophotometry	H_2O_2	0.5 – $30 \text{ mmol}\cdot\text{L}^{-1}$	[12]
Colorimetry	H_2O_2 , HRP, phenol, 4-aminoantipyrene	0.175 – $0.70 \text{ mmol}\cdot\text{L}^{-1}$	[13]
Spectrofluorimetry	H_2O_2 , HRP, homovanillic acid	0.02 – $0.3 \text{ mmol}\cdot\text{L}^{-1}$	[14]
Chemiluminescence	H_2O_2 , TCPO, 9,10-diphenylanthracene	9.0 – $72.0 \mu\text{mol}\cdot\text{L}^{-1}$	[16]
SERS	SiO_2 , gold nanoparticles	0 – $200 \mu\text{mol}\cdot\text{L}^{-1}$	[19]
Fluorescence	H_2O_2 , Fe^{2+} , gold nanoclusters	0.5 – $10 \mu\text{mol}\cdot\text{L}^{-1}$	This work

Acknowledgements The work was supported by the National Natural Science Foundation of China (No. 21675107) and Fundamental Research Funds for the Central Universities (Grant No. GK201603029).

Compliance with ethical standards The author (s) declare that they have no competing interests.

References

- Circu ML, Aw TY (2010) Reactive oxygen species, cellular redox systems, and apoptosis. *Free Radic Biol Med* 48(6):749–762
- Gorlach A, Dimova EY, Petry A, Martinez-Ruiz A, Hermansanz-Agustin P, Rolo AP, Palmeira CM, Kietzmann T (2015) Reactive oxygen species, nutrition, hypoxia and diseases: problems solved? *Redox Biol* 6:372–385
- Zuo L, Zhou T, Pannell BK, Ziegler AC, Best TM (2015) Biological and physiological role of reactive oxygen species—the good, the bad and the ugly. *Acta Physiol* 214(3):329–348
- Mittal M, Siddiqui MR, Tran K, Reddy SP, Malik AB (2014) Reactive oxygen species in inflammation and tissue injury. *Antioxid Redox Signal* 20(7):1126–1167
- Slimen IB, Najar T, Ghram A, Dabbebi H, Mrad MB, Abdrabbah M (2014) Reactive oxygen species, heat stress and oxidative-induced mitochondrial damage. A review *Int J Hyperther* 30(7):513–523
- Chen L, Wu N, Sun B, Su H, Ai S (2013) Colorimetric detection of peroxynitrite-induced DNA damage using gold nanoparticles, and on the scavenging effects of antioxidants. *Microchim Acta* 180(7–8):573–580
- Winterbourn CC (2013) The biological chemistry of hydrogen peroxide. *Methods Enzymol* 528:3–25
- Rhee SG (2006) H₂O₂, a necessary evil for cell signaling. *Science* 312(5782):1882–1883
- Veal E, Day A (2011) Hydrogen peroxide as a signaling molecule. *Antioxid Redox Signal* 15(1):147–151
- Halliwell B, Gutteridge JM (1984) Oxygen toxicity, oxygen radicals, transition metals and disease. *Biochem J* 219(1):1–14
- Melnikova L, Pospiskova K, Mitrova Z, Kopcansky P, Afarik I (2014) Peroxidase-like activity of magnetoferritin. *Microchim Acta* 181(3):295–301
- Magalhães LM, Segundo MA, Reis S, Lima JLFC (2008) Methodological aspects about in vitro evaluation of antioxidant properties. *Anal Chim Acta* 613(1):1–19
- Fernando CD, Soysa P (2015) Optimized enzymatic colorimetric assay for determination of hydrogen peroxide (H₂O₂) scavenging activity of plant extracts. *Methods X* 2:283–291
- Pazdziuch-Czochra M, Widenska A (2002) Spectrofluorometric determination of hydrogen peroxide scavenging activity. *Anal Chim Acta* 452(2):177–184
- Halliwell B (1978) Lignin synthesis: the generation of hydrogen peroxide and superoxide by horseradish peroxidase and its stimulation by manganese (II) and phenols. *Planta* 140(1):81–88
- Amous A, Petrakis C, Makris DP, Kefalas P (2002) Peroxyoxalate chemiluminescence-based assay for the evaluation of hydrogen peroxide scavenging activity employing 9, 10-diphenylanthracene as the fluorophore. *J Pharmacol Toxicol Methods* 48(3):171–177
- Mansouri A, Makris DP, Kefalas P (2005) Determination of hydrogen peroxide scavenging activity of cinnamic and benzoic acids employing a highly sensitive peroxyoxalate chemiluminescence-based assay: structure-activity relationships. *J Pharm Biomed Anal* 39(1–2):22–26
- Li H, Ma XY, Dong J, Qian WP (2009) Development of methodology based on the formation process of gold nanoshells for detecting hydrogen peroxide scavenging activity. *Anal Chem* 81(21):8916–8922
- Rao YY, Chen QF, Dong J, Qian WP (2011) Growth-sensitive 3D ordered gold nanoshells precursor composite arrays as SERS nanoprobe for assessing hydrogen peroxide scavenging activity. *Analyst* 136(4):769–774
- Chen LY, Wang CW, Yuan ZQ, Chang HT (2015) Fluorescent gold nanoclusters: recent advances in sensing and imaging. *Anal Chem* 87(1):216–229
- Chaudhari K, Xavier PL, Pradeep T (2011) Understanding the evolution of luminescent gold quantum clusters in protein templates. *ACS Nano* 5(11):8816–8827
- Xie JP, Zheng YG, Ying JY (2009) Protein-directed synthesis of highly fluorescent gold nanoclusters. *J Am Chem Soc* 131(3):888–889
- Liu CL, Wu HT, Hsiao YH, Lai CW, Shih CW, Peng YK, Tang KC, Chang HW, Chien YC, Hsiao JK, Cheng JT, Chou PT (2011) Insulin-directed synthesis of fluorescent gold nanoclusters: preservation of insulin bioactivity and versatility in cell imaging. *Angew Chem Int Ed* 50(31):7056–7060
- Kawasaki H, Hamaguchi K, Osaka I, Arakawa R (2011) pH-dependent synthesis of pepsin-mediated gold nanoclusters with blue green and red fluorescent emission. *Adv Funct Mater* 21(18):3508–3515
- Wen F, Dong YH, Feng L, Wang S, Zhang SC, Zhang XR (2011) Horseradish peroxidase functionalized fluorescent gold nanoclusters for hydrogen peroxide sensing. *Anal Chem* 83(4):1193–1196
- Zhang GM, Qiao YY, Xu T, Zhang CH, Zhang Y, Shi LH, Shuang SM, Dong C (2015) Highly selective and sensitive nanoprobe for cyanide based on gold nanoclusters with red fluorescence emission. *Nanoscale* 7(29):12666–12672
- Bankar SB, Bule MV, Singhal RS, Ananthanarayan L (2009) Glucose oxidase—an overview. *Biotechnol Adv* 27(4):489–501
- Xia XD, Long YF, Wang JX (2013) Glucose oxidase-functionalized fluorescent gold nanoclusters as probes for glucose. *Anal Chim Acta* 772:81–86
- Shamsipur M, Molaabasi F, Shanehsaz M, Moosavi-Movahedi AA (2015) Novel blue-emitting gold nanoclusters confined in human hemoglobin, and their use as fluorescent probes for copper (II) and histidine. *Microchim Acta* 182(5):1131–1141
- Zheng J, Petty JT, Dickson RM (2003) High quantum yield blue emission from water-soluble Au₈ nanodots. *J Am Chem Soc* 125(26):7780–7781
- Esposito R, Delfino I, Lepore M (2013) Time-resolved flavin adenine dinucleotide fluorescence study of the interaction between immobilized glucose oxidase and glucose. *J Fluoresc* 23(5):947–955
- Zheng J, Zhang CW, Dickson RM (2004) Highly fluorescent, water-soluble, size-tunable gold quantum dots. *Phys Rev Lett* 93(7):077402
- Wei H, Wang ZD, Yang LM, Tian SL, Hou CJ, Lu Y (2010) Lysozyme-stabilized gold fluorescent cluster: synthesis and application as Hg²⁺ sensor. *Analyst* 135(6):1406–1410
- Jin LH, Shang L, Guo SJ, Fang YX, Wen D, Wang L, Yin JY, Dong SJ (2011) Biomolecule-stabilized Au nanoclusters as a fluorescence probe for sensitive detection of glucose. *Biosens Bioelectron* 26(5):1965–1969